



Contents lists available at ScienceDirect

International Journal of Applied Earth Observations and Geoinformation

journal homepage: www.elsevier.com/locate/jag

Hyperspectral indices optimization algorithms for estimating canopy nitrogen concentration in potato (*Solanum tuberosum* L.)

Haibo Yang^a, Fei Li^{a,*}, Yuncai Hu^b, Kang Yu^c^a Inner Mongolia Key Laboratory of Soil Quality and Nutrient Resource, College of Grassland, Resources and Environment, Inner Mongolia Agricultural University, Hohhot, Inner Mongolia 010011, China^b Chair of Plant Nutrition, Department of Plant Sciences, Technical University of Munich, Emil-Ramann-Str. 2, D-85354 Freising, Germany^c Department Life Science Engineering, School of Life Sciences, Technical University of Munich, 85354 Freising, Germany

ARTICLE INFO

Keywords:

Hyperspectral indices
Wavebands optimum
Formula formats
Canopy nitrogen concentration
Potato

ABSTRACT

Many empirical models based on hyperspectral indices (HIs) have been developed to estimate nitrogen (N) status of crops. However, most of the researches by far focused on the identification of sensitive bands of HIs, and have not identified the importance of formula formats to achieve their best performance. The current study aimed to investigate the response of band optimization and formula formats to canopy N concentration (CNC) of potato (*Solanum tuberosum* L.) plants, and to verify the performance of HIs through optimized algorithms based on a multi-site and -year study. Three field experiments involving different potato cultivars with 3–6 N rates were conducted from 2014 to 2016 in Inner Mongolia, China. The band optimization HIs were first tested using a simulated dataset by the PROSAIL model and validation dataset from farmers' fields. Results showed that the optimized HIs generally had more robust performances for CNC prediction than the published indices. The optimized HIs explained 56%–74% of the variations in potato CNC in contrast with 3%–53% variation of HIs by 16%–71%. The choice of the formula formats affected the explanatory power of the optimized HIs by 3%–18%. Our study found that both the performance of HIs and the position of the sensitive bands were greatly influenced by formula formats. The results from the evaluation of noise equivalent that independent from farmers' field and PROSAIL model showed that the best performance was from Opt-CCCI. The central sensitive bands of Opt-CCCI were found at 600, 582, 650 nm. Opt-mRER also exhibited well in noise equivalent and independent validation from farmers' field, while they could not be verified with the PROSAIL model because of the absence of the wavebands from 340 to 400 nm. Optimization for HIs indicates that there will be a great potential to improve the use of hyperspectral sensing for the estimation of field crops CNC.

1. Introduction

Potato is the fourth most important crop in the world in terms of global production quantity (Wang et al., 2018, 2019). China is the largest potato producing country globally in terms of area and production (FAO, 2019). Therefore, potato yield plays a critical role in food security in China. In order to enhance potato yield, excessive nitrogen (N) fertilization often occurs in potato growing regions (Tang et al., 2021). However, because potato (*Solanum tuberosum* L.) crops are characterized with a shallower root system, N fertilizer is needed to apply several times to meet the N demands during their growing season (Goffart et al., 2008). Furthermore, excessive N fertilization results in

negative environmental impacts (Tang et al., 2021), and thus optimizing N management is important to maintain a high potato yield and sustainable environment in China.

Optimizing N fertilization management requires timely and accurate monitoring N status of field crops (Zhao et al., 2012). Currently, many hyperspectral indices (HIs) based on canopy or leaf reflectance spectra have been proposed, and widely used to predict crop canopy N status (Li et al., 2010). This is because HIs enhance spectral features sensitive to vegetation biochemical or biophysical properties, while reducing disturbance by using specific formula formats that consist of several sensitive bands (Glenn et al., 2008). Although waveband combinations and formula formats are able to improve the performance of HIs for

* Corresponding author.

E-mail address: lifei@imau.edu.cn (F. Li).

<https://doi.org/10.1016/j.jag.2021.102416>

Received 13 May 2021; Received in revised form 13 June 2021; Accepted 14 June 2021

Available online 3 July 2021

0303-2434/© 2021 The Author(s).

Published by Elsevier B.V. This is an open access article under the CC BY-NC-ND license

(<http://creativecommons.org/licenses/by-nc-nd/4.0/>).

Table 1
Algorithms corresponding to the hyperspectral indices used in this work.

Spectral indices	Abbreviation	Formulas	References	Algorithms
Two-band spectral indices				
Ratio vegetation index	RVI	R_{800}/R_{670}	Jordan, 1969	$R_{3,1}/R_{3,2}$
Normalized difference vegetation index	NDVI	$(R_{800}-R_{680})/(R_{800} + R_{680})$	Rouse et al., 1974	$(R_{3,1}-R_{3,2})/(R_{3,1} + R_{3,2})$
Different vegetation index	DVI	$R_{800}-R_{680}$	Tucker, 1979	$R_{3,1}-R_{3,2}$
Soil adjusted vegetation index	SAVI	$1.5 \times (R_{800}-R_{670})/(R_{800} + R_{670} + 0.5)$	Huete, 1988	$1.5 \times (R_{3,1}-R_{3,2})/(R_{3,1} + R_{3,2} + 0.5)$
Modified soil-adjusted vegetation index	MSAVI	$0.5 \times (2 \times R_{810} + 1 - ((2 \times R_{810} + 1)^2 \cdot 8 \times (R_{810}-R_{670})^{0.5}))$	Qi et al., 1994	$0.5 \times (2 \times R_{3,1} + 1 - ((2 \times R_{3,1} + 1)^2 \cdot 8 \times (R_{3,1}-R_{3,2})^{0.5}))$
The renormalized difference vegetation index	RDVI	$(R_{800}-R_{670})/\sqrt{R_{800} + R_{670}}$	Roujean and Breon, 1995	$(R_{3,1}-R_{3,2})/\sqrt{R_{3,1} + R_{3,2}}$
Optimized soil-adjusted vegetation index	OSAVI	$(R_{800}-R_{670})/(1 + 0.16)/(R_{800} + R_{670} + 0.16)$	Rondeaux et al., 1996	$1.16 \times (R_{3,1}-R_{3,2})/(R_{3,1} + R_{3,2} + 0.16)$
Red edge chlorophyll index	CI _{red-edge}	$(R_{780}-R_{710})/R_{710}$	Gitelson et al., 2003	$(R_{3,1} + R_{3,2})/R_{3,2}$
Optimal vegetation index*	Vlopt	$(1 + 0.45) \times ((R_{800})^2 + 1)/(R_{670} + 0.45)$	Reyniers et al., 2006	$(1 + 0.45) \times ((R_{3,1})^2 + 1)/(R_{3,2} + 0.45)$
Three-band spectral indices				
Three-band ratio spectral index (TRSI	$R_{675}/(R_{700} \times R_{650})$	Chappelle et al., 1992	$R_{3,1}/(R_{3,2} \times R_{3,3})$
Structural insensitive pigment index	SIPI	$(R_{800}-R_{445})/(R_{800}-R_{680})$	Peñuelas et al., 1995	$(R_{3,1}-R_{3,2})/(R_{3,1}-R_{3,3})$
Modified chlorophyll absorption reflectance index	MCARI	$[(R_{700}-R_{670})-0.2 \times (R_{700}-R_{550})] \times (R_{700}/R_{670})$	Daughtry et al., 2000	$[(R_{3,1}-R_{3,2})-0.2 \times (R_{3,1}-R_{3,3})] \times (R_{3,1}/R_{3,2})$
Triangle vegetation index	TVI	$0.5 \times (120 \times (R_{750}-R_{550})-200 \times (R_{670}-R_{550}))$	Broge and leblanc, 2001	$0.5 \times (120 \times (R_{3,1}-R_{3,2})-200 \times (R_{3,3}-R_{3,2}))$
Transformed chlorophyll absorption reflectance index	TCARI	$3 \times [(R_{700}-R_{670})-0.2 \times (R_{700}-R_{550})] \times (R_{700}/R_{670})$	Haboudane et al., 2002	$3 \times [(R_{3,1}-R_{3,2})-0.2 \times (R_{3,1}-R_{3,3})] \times (R_{3,1}/R_{3,2})$
Plant senescence reflectance index	PSRI	$(R_{680}-R_{500})/R_{750}$	Merzlyak et al., 1999	$(R_{3,1}-R_{3,2})/R_{3,3}$
Modified Red-edge Ratio	mSR705	$(R_{750}-R_{445})/(R_{705}-R_{445})$	Sims and Gamon, 2002	$(R_{3,1}-R_{3,2})/(R_{3,3}-R_{3,2})$
Modified red-edge normalized difference	mND705	$(R_{750}-R_{705})/(R_{750} + R_{705}-2 \times R_{445})$	Sims and Gamon, 2002	$(R_{3,1}-R_{3,2})/(R_{3,1} + R_{3,2}-2 \times R_{3,3})$

Table 1 (continued)

Spectral indices	Abbreviation	Formulas	References	Algorithms
vegetation index				
The MERIS terrestrial chlorophyll index	MTCI	$(R_{750}-R_{710})/(R_{710}-R_{680})$	Dash and Curran, 2004	$(R_{3,1}-R_{3,2})/(R_{3,2}-R_{3,3})$
Modified triangular vegetation index 1	MTVII	$1.2 \times [1.2 \times (R_{800}-R_{550})-2.5 \times (R_{670}-R_{550})]$	Haboudane et al., 2004	$1.2 \times [1.2 \times (R_{3,1}-R_{3,2})-2.5 \times (R_{3,3}-R_{3,2})]$
Double-peak canopy nitrogen index	DCNI	$(R_{720}-R_{700})/(R_{700}-R_{670})/(R_{720}-R_{670} + 0.03)$	Chen et al., 2010	$(R_{3,1}-R_{3,2})/(R_{3,2}-R_{3,3})/(R_{3,1}-R_{3,3} + 0.03)$
Blue nitrogen index 1	BNI1	$R_{434}/(R_{496} + R_{401})$	Tian et al., 2011	$R_{3,1}/(R_{3,2} + R_{3,3})$
Blue nitrogen index 2	BNI2	$(R_{498} + R_{413})/R_{442}$	Tian et al., 2011	$(R_{3,1} + R_{3,2})/R_{3,3}$
Modified normalized difference vegetation index	mNDVI _{blue}	$(R_{924}-R_{703} + 2 \times R_{423})/(R_{924} + R_{703}-2 \times R_{423})$	Wang et al., 2012	$(R_{3,1}-R_{3,2} + 2 \times R_{3,3})/(R_{3,1} + R_{3,2}-2 \times R_{3,3})$
Double-peak nitrogen index	NDDA	$(R_{755} + R_{680}-2 \times R_{705})/(R_{755}-R_{680})$	Feng et al., 2014	$(R_{3,1} + R_{3,2}-2 \times R_{3,3})/(R_{3,1}-R_{3,2})$
Modified red-edge ratio	mRER	$(R_{759}-1.8 \times R_{419})/(R_{742}-1.8 \times R_{419})$	Feng et al., 2015	$(R_{3,1}-1.8 \times R_{3,2})/(R_{3,3}-1.8 \times R_{3,2})$
Combined spectral indices				
Canopy chlorophyll content index	CCCI	$(NDRE-NDRE_{MIN})/(NDRE_{MAX}-NDRE_{MIN})$	Fitzgerald et al., 2010	$(NDRE-NDRE_{MIN})/(NDRE_{MAX}-NDRE_{MIN})$
Nitrogen planar domain index	NPDI	$(CI_{red\ edge}-CI_{red\ edge\ MIN})/(CI_{red\ edge\ MAX}-CI_{red\ edge\ MIN})$	Li et al., 2012	$(CI_{red\ edge}-CI_{red\ edge\ MIN})/(CI_{red\ edge\ MAX}-CI_{red\ edge\ MIN})$
MCARI/OSAVI	MCARI/OSAVI	MCARI/OSAVI	Zarco-Tejada et al., 2004	MCARI/OSAVI
Canopy Chlorophyll Inversion Index	CCII	TCARI/OSAVI	Haboudane et al., 2002	TCARI/OSAVI

The R was the abbreviation of reference in formulas and algorithms; * The Vlopt was defined the optimized vegetative index in the previous study, we adopt the abbreviation of Vlopt, but in the current study, the combination of bands was further optimized form 340–1050 nm.

Table 2
The ranges of the input parameters for the PROSAIL model.

Parameter	Min.	Max.
Leaf structure parameter	1	2
Equivalent water thickness (cm)	0.005	0.03
Leaf mass per area (g/cm ²)	0.004	0.01
leaf area index (m ² /m ²)	1	6
Average leaf angle (deg)	30	70
Soil moisture parameter	0	1
Hot spot size parameter (deg)	0.05	1
Solar zenith angle (deg)	30	60
view zenith angle (deg)	0	0
View azimuth angle (deg)	0	0

estimating crop N status, their performances are influenced by sites, years, crop growth stages and cultivars (Zhang et al., 2020). Consequently, a large number of new band combinations and formula formats

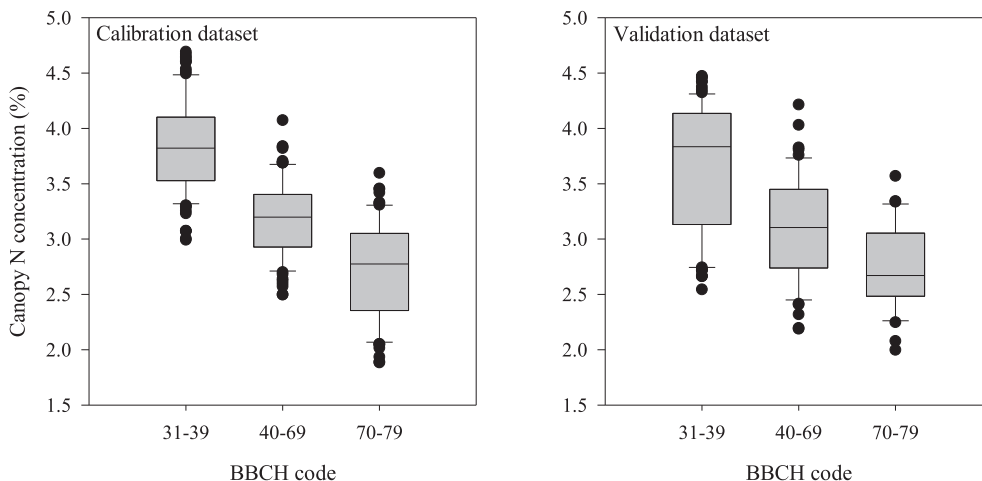


Fig. 1. Temporal variation of the canopy nitrogen (N) concentration at (a) experimental field and (b) farmers’ field. The distribution is characterized by box-and-whisker plots, where the boxes show the 25th and 75th percentiles and the whiskers the 10th and the 90th percentiles. The median is represented by the line in the box and is provided as a number above the box plot. BBCH code is a scale used to identify the phenological development stages of a plant (Lancashire, 1991).

Published Spectral indices	Wavebands (nm)			Coefficient of determination (R^2)											
	$R_{\lambda,1}$	$R_{\lambda,2}$	$R_{\lambda,3}$	0.0	0.1	0.2	0.3	0.4	0.5	0.6					
RVI	800	670		[Bar chart showing R² ≈ 0.05]											
NDVI	800	680		[Bar chart showing R² ≈ 0.05]											
DVI	800	680		[Bar chart showing R² ≈ 0.22]											
SAVI	800	670		[Bar chart showing R² ≈ 0.05]											
MSAVI	810	670		[Bar chart showing R² ≈ 0.05]											
RDVI	800	670		[Bar chart showing R² ≈ 0.22]											
OSAVI	800	670		[Bar chart showing R² ≈ 0.05]											
CI _{red-edge}	780	710		[Bar chart showing R² ≈ 0.35]											
VI _{opt}	800	670		[Bar chart showing R² ≈ 0.12]											
TRSI	675	700	650	[Bar chart showing R² ≈ 0.45]											
SIPI	800	445	680	[Bar chart showing R² ≈ 0.02]											
MCARI	700	670	550	[Bar chart showing R² ≈ 0.18]											
TVI	750	670	550	[Bar chart showing R² ≈ 0.18]											
TCARI	700	670	550	[Bar chart showing R² ≈ 0.05]											
PSRI	680	500	750	[Bar chart showing R² ≈ 0.52]											
mSR705	750	445	705	[Bar chart showing R² ≈ 0.42]											
mND705	750	705	445	[Bar chart showing R² ≈ 0.48]											
MTCI	750	710	680	[Bar chart showing R² ≈ 0.45]											
MTVI1	800	550	670	[Bar chart showing R² ≈ 0.18]											
DCNI	720	700	670	[Bar chart showing R² ≈ 0.22]											
BNI1	434	496	401	[Bar chart showing R² ≈ 0.48]											
BNI2	498	413	442	[Bar chart showing R² ≈ 0.55]											
mNDVI _{I_{blue}}	924	703	423	[Bar chart showing R² ≈ 0.55]											
NDDA	755	680	705	[Bar chart showing R² ≈ 0.52]											
mRER	759	724	419	[Bar chart showing R² ≈ 0.05]											
CCCI	800	720	680	[Bar chart showing R² ≈ 0.42]											
NPDI	958	696	578	[Bar chart showing R² ≈ 0.18]											
MCARI/OSAVI	700 (800)	670	550	[Bar chart showing R² ≈ 0.22]											
CCII	700 (800)	670	550	[Bar chart showing R² ≈ 0.05]											

Fig. 2. Description of published spectral indices bands and the relationships between published spectral indices and potato canopy nitrogen concentration.

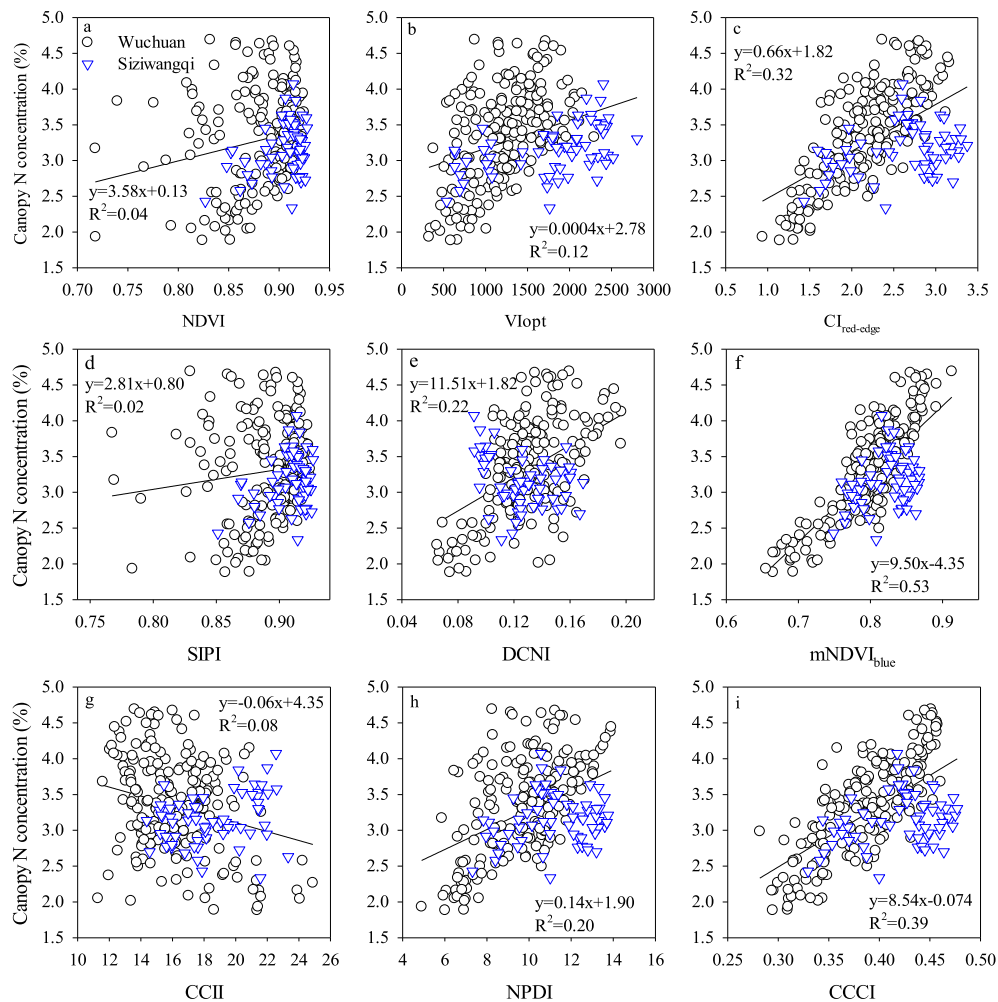


Fig. 3. Relationships between the canopy nitrogen (N) concentration and published HIs (a) NDVI, (b) VI_{opt}, (c) CI_{red-edge}, (d) SIPI, (e) DCNI, (f) mNDVI_{blue}, (g) CCII, (h) NPDI and (i) CCCL.

have been developed to increase HIs performance and universality. In particular, the rapid development of hyperspectral remote sensing technology with high-resolution hyperspectral instrumentations provides more potential wavebands for optimizing the published HIs (Adão et al., 2017). Therefore, identifying the response of sensitive bands and formula formats for the optimized indices allows to further improve the feasibility, to develop more robust and accurate HIs for estimation of the crop N status.

Simple ratio- and normalized difference-based HIs are the basic formula formats of HIs (Rouse et al., 1974; Jordan, 1969), and are commonly used to derive the vegetative characteristics. However, many studies have shown that the degree of dispersion of biomass prediction models increases under the low coverage conditions (Daughtry et al., 2000) and/or that models lose sensitivity to moderate-to-high of leaf area index (Erdle et al., 2011), CNC (Prey et al., 2019) and leaf chlorophyll content (Yu et al., 2014). In order to overcome these problems, a number of formula formats of HIs have been developed to enhance the robustness of HIs in predicting vegetation properties. Huete et al. (1988) introduced a constant (L) based on soil reflectance and proposed a soil-adjusted vegetation index, which nearly eliminates soil-induced variations in NDVI. Subsequently, after the formula of the SAVI was further modified, the new modified soil adjusted vegetation index (MSAVI) and optimized soil-adjusted vegetation index (OSAVI) have been constructed (Qi et al., 1994; Rondeaux et al., 1996). In order to overcome the saturation problem of HIs, Gitelson et al. (2004) modified the NDVI with a weighting coefficient that increased the sensitivity of the NDVI to a

high leaf area index (LAI). Furthermore, Sims and Gamon (2002) modified the NDVI and RVI by adding a reference waveband (R₄₄₅), i.e., the new three-band HIs mSR705 and mND705 that significantly improve the sensitivity of NDVI and RVI at higher chlorophyll levels. Based on the concept of “Planar domain index” as proposed by Clarke et al. (2001), the Canopy Chlorophyll Content Index (CCCI) and the Nitrogen Planar Domain Index (NPDI) was derived by using two indices: NDRE/CI_{red edge} sensitive to the desired quality of canopy N and NDVI sensitive to the relative proportion to the whole canopy cover. The combined HIs overcome the effects of canopy structure and coverage on HIs performance (Li et al., 2014c; Fitzgerald et al., 2010).

With the development of high resolutions for spectral instrumentations, the number of bands obtained by remote sensing is increasing, and the bandwidth is getting narrower (Honkavaara et al., 2013). However, the problem is how to identify the best band combinations in a given special formula format of HIs. A popular solution is to calculate all possible band combination according to established HIs formula formats (Verrelst et al., 2019). Thenkabail et al. (2000) analyzed all band combinations for NDVI from 350 nm to 1050 nm and the optimized NDVI could explain 64% to 88% variability in different crop biophysical variables. Subsequently, the band-optimized HIs have been widely reported. Numerous studies on maize, wheat, rice, cotton and barley have demonstrated that compared with the published HIs, the band optimized HIs could increase the explanatory power of canopy N concentration by 19%–43% (Kasim et al., 2018; Li et al., 2010, 2014a, 2014c; Yu et al., 2013; Stroppiana et al., 2009). Therefore, optimizing

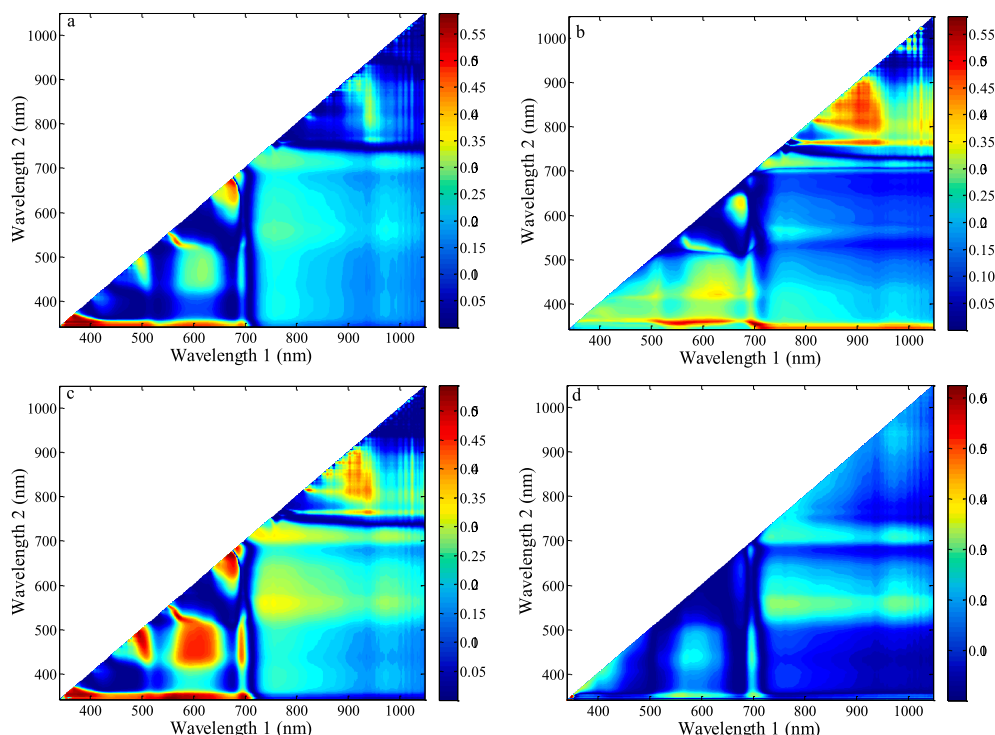


Fig. 4. The contour diagram showing the R^2 for the relationships between the canopy nitrogen concentration and narrow band (a) DVI, (b) MSAVI, (c) RDVI and (d) VLOpt that were calculated from all possible two band combinations in the range of 340–1050 nm.

the bands for HIs is an essential step of ensuring the estimation accuracy.

To date, CNC is an effective indicator for reflecting crop N nutrient status, especially when N nutrition index (NNI) is used to determine whether a crop suffers from N deficiency or sufficiency (Le Maire et al., 2008). Remotely and accurately quantifying the CNC in crops is essential for crop nitrogen management (Chen et al., 2010). However, many studies focus on comparing the performance between different published HIs and developed new band optimized HIs. To some extent, the influence of HIs formula formats on the estimation accuracy has been ignored. Therefore, the objectives of the present study were: (1) to identify the contribution of band optimization and formula formats in estimation potato CNC, (2) to assess the performances of optimized HIs, and (3) to develop the feasible and robust HIs for estimating CNC in potato plants.

2. Material and methods

2.1. Study sites

The experiments were conducted in Wuchuan (41°54'47" N, 111°27'4" E) and Siziwangqi Country (41°31'59" N, 111°42'24" E) in Inner Mongolia, China. The climate is middle temperate arid and semi-arid continental monsoon, i.e., with cold winters and cool summers. The main crops in this area are potato, sunflower (*Helianthus annuus* L.) and oats (*Avena sativa* L.). The precipitation and temperature in potato growing season varied with a range of 350–370 mm and 10–26 °C, respectively, from 2014 to 2016.

2.2. Experimental design

There were three calibration experiments with different N levels to establish the relationships between HIs and the canopy N concentration. Experiment 1 including 6 N rates (0, 83, 135, 165, 180 and 250 kg N ha⁻¹) and potato cultivar Kexin1 and Experiment 2 including 6 N rates (0, 90, 144, 180 and 270 kg N ha⁻¹) and cultivar Xiapodi was carried out in Wuchuan County in 2014 and 2015, respectively. In 2016,

Experiment 3 including 3 N rates, i.e., the control (no N applied), optimum N rate based on the residual soil mineral N previously assessed using a quick-test method (Schmidhalter, 2005) and conventional N rate from farmers' practices, and Holland 14 potato cultivar was conducted in Siziwangqi. Nitrogen fertilizer as fertigation was applied at five growth stages. The plot size was 9 × 9 m for Exp. 1 and Exp. 2, and 9 × 12 m for Exp. 3. There was a completely random block design with four replicates in all experimental plots.

Validation experiments were undertaken to test the stability and robustness of the optimized HIs for estimating the CNC in different farmers' fields near the sites of Exp. 1, 2 and 3 from 2014 to 2016. Local cultivars were used, and the fields were managed by the farmers. The different farmers' fields were used as replications.

2.3. Data collection

2.3.1. Spectral measurements

The canopy reflectance of potato was measured with a handheld spectrometer (Handy-Spec, tec5 AG, Germany) under a clear day conditions between 10:00 a.m. and 2:00 p.m. in the critical growing season from mid-July to the end of August, which corresponded to the BBCH code 31–79 (Lancashire et al., 1991). The sensor measures at 256 bands within a spectral range of 300–1150 nm, and it has a bandwidth of 3.3 nm. Canopy reflectance data were collected by holding the sensor in a nadir position approximately 0.5–0.8 m above the canopy and walking a distance of 4–6 m with a constant speed along the potato ridges across each plot.

2.3.2. Plant sampling and measurements

The above-ground plants in two 1-m consecutive rows of potato in the spectrometer-scanned locations of each plot were sampled. Chopping samples and then mixing them to take 400–600 g sub-samples. All sub-samples were oven-dried at 70 °C to constant weight, and then weighted and ground for chemical analysis later. The CNC was determined by the Kjeldahl-N analysis. A total of 267 valid data were collected as the calibration dataset in the experimental fields from 2014

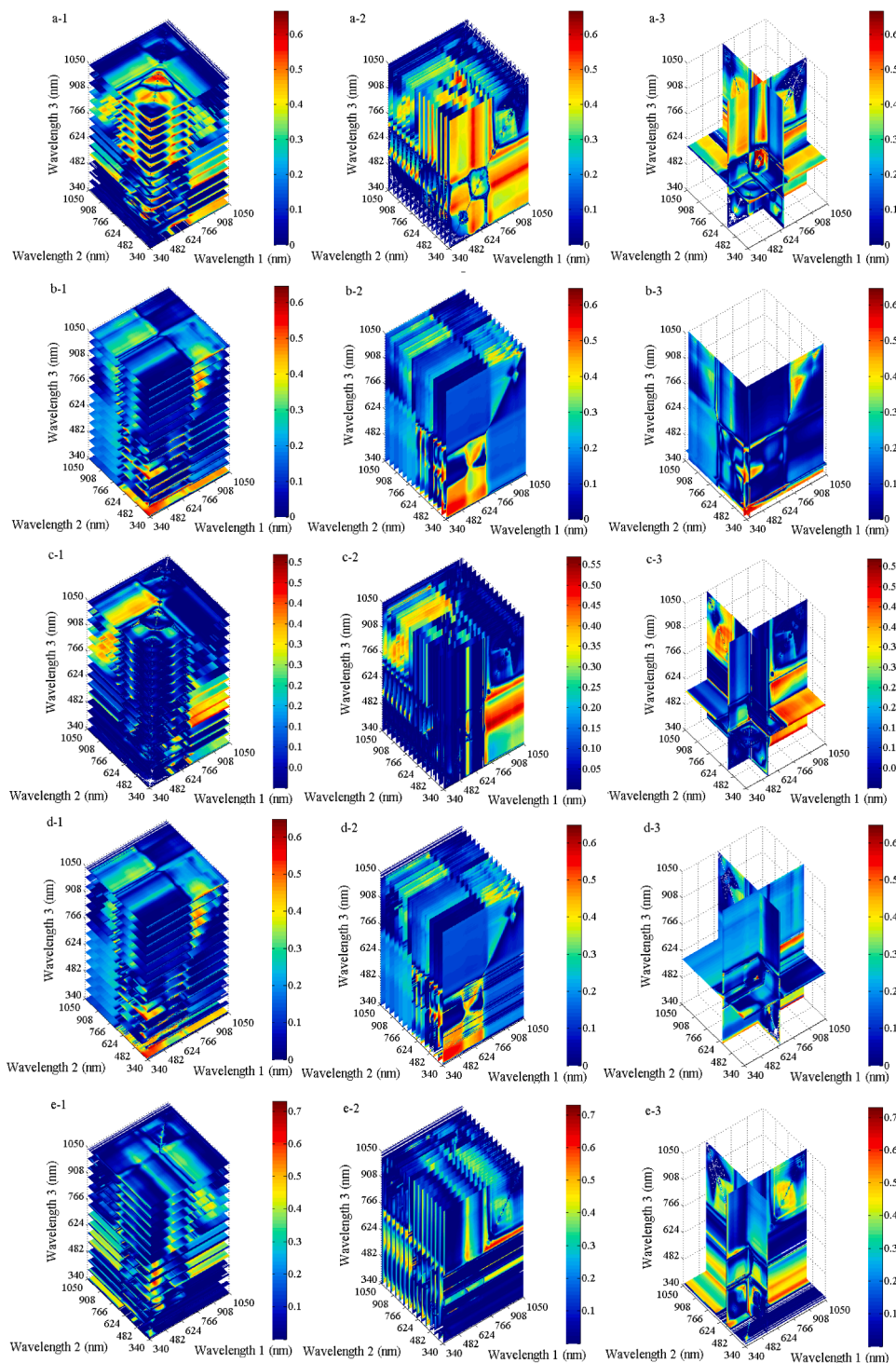


Fig. 5. Slice maps showing of R^2 for relationships between the canopy nitrogen concentration (CNC) and the single three-band spectral indices (a) SIPI, (b) MCARI (c) DCNI and combined spectral indices (d) Opt-CCII (e) Opt-NPDI that were calculated for all possible three-band combination in the range of 340–1050 nm in the entire growth stage (1: horizontal slice map, 2: vertical slice map and 3: optimum slice map).

to 2016, and 178 independent validation data from the farmers’ fields were used to validate the performance of different HIs.

2.4. Hyperspectral indices

Spectral indices were by far the classical and commonly used method of variable estimation parameters. In order to investigate the influence of different types of HIs algorithms on estimating CNC of potato, 29

published HIs were chosen in this work (Table 1). To improve the performance of the published HIs, the band combinations of published HIs were optimized by considering all possible combinations of two and three wavelengths from 340 to 1050 nm under the specific formula formats. The two- and three-dimensional contour and slice maps of the coefficients of determination were constructed between optimized HIs and CNC using MATLAB 7.0.

Optimized spectral indices	Optimized bands (nm)			Coefficient of determination (R^2)								
	R_{λ_1}	R_{λ_2}	R_{λ_3}	0.0	0.1	0.2	0.3	0.4	0.5	0.6	0.7	0.8
Opt-RVI	492	494		[Bar chart showing R² ≈ 0.65]								
Opt-NDVI	492	494		[Bar chart showing R² ≈ 0.65]								
Opt-DVI	352	386		[Bar chart showing R² ≈ 0.65]								
Opt-SAVI	492	494		[Bar chart showing R² ≈ 0.65]								
Opt-MSAVI	704	352		[Bar chart showing R² ≈ 0.65]								
Opt-RDVI	342	564		[Bar chart showing R² ≈ 0.55]								
Opt-OSAVI	492	494		[Bar chart showing R² ≈ 0.65]								
Opt- $CI_{red-edge}$	492	494		[Bar chart showing R² ≈ 0.65]								
Opt-VIopt	348	350		[Bar chart showing R² ≈ 0.65]								
Opt-TRSI	554	360	748	[Bar chart showing R² ≈ 0.60]								
Opt-SIPI	582	584	658	[Bar chart showing R² ≈ 0.70]								
Opt-MCARI	366	378	400	[Bar chart showing R² ≈ 0.65]								
Opt-TVI	366	390	380	[Bar chart showing R² ≈ 0.65]								
Opt-TCARI	366	378	398	[Bar chart showing R² ≈ 0.65]								
Opt-PSRI	562	352	532	[Bar chart showing R² ≈ 0.75]								
Opt-mSR705	582	584	658	[Bar chart showing R² ≈ 0.75]								
Opt-mND705	582	584	658	[Bar chart showing R² ≈ 0.75]								
Opt-MTCI	582	584	658	[Bar chart showing R² ≈ 0.75]								
Opt-MTVI1	388	366	380	[Bar chart showing R² ≈ 0.65]								
Opt-DCNI	558	556	532	[Bar chart showing R² ≈ 0.60]								
Opt-BNI1	562	534	354	[Bar chart showing R² ≈ 0.75]								
Opt-BNI2	532	352	564	[Bar chart showing R² ≈ 0.75]								
Opt-mNDVI _{blue}	894	342	924	[Bar chart showing R² ≈ 0.75]								
Opt-NDDA	582	658	584	[Bar chart showing R² ≈ 0.75]								
Opt-mRER	352	536	562	[Bar chart showing R² ≈ 0.75]								
Opt-CCCI	600	582	650	[Bar chart showing R² ≈ 0.70]								
Opt-NPDI	352	564	536	[Bar chart showing R² ≈ 0.75]								
Opt-MCARI/OSAVI	508	512	522	[Bar chart showing R² ≈ 0.70]								
Opt-CCII	582	594	650	[Bar chart showing R² ≈ 0.70]								

Fig. 6. Description of optimal bands and the relationships between optimized spectral indices and potato canopy nitrogen concentration.

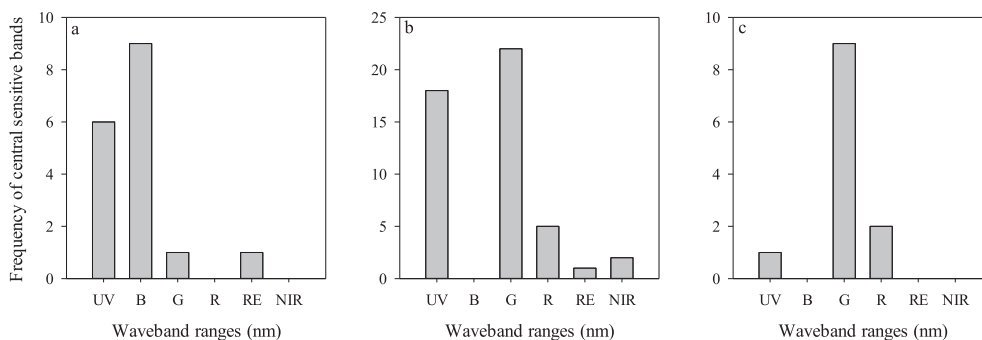


Fig. 7. Frequency of sensitive bands with (a) two-band HIs, (b) three-band HIs, (c) combined HIs and (ultraviolet radiation (UV) range: 340–400 nm, blue light (B) range: 450–520 nm, green light (G) range: 520–600 nm, red light (R) range: 600–690 nm, red edge radiation (RE): 690–750 nm, near infrared radiation (NIR) range: 750–1050 nm).

2.5. Evaluation of optimized HIs

2.5.1. Sensitive evaluation

The linear empirical models between optimized HIs and CNC were

constructed according to the optimal sensitive bands. The sensitivity of the different optimized HIs in deriving CNC of potato was tested using the Noise Equivalent (NE) method (Vin and Gitelson, 2005) based on following equation:

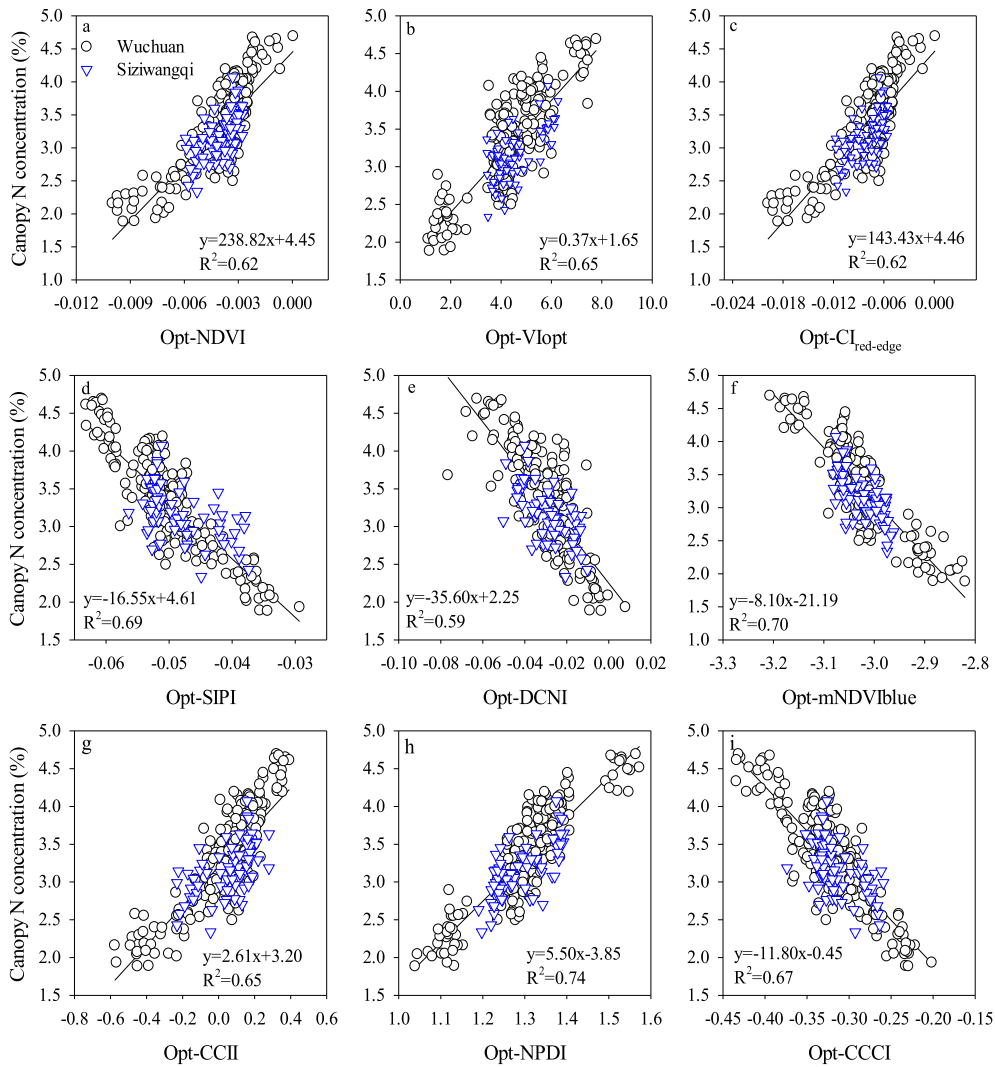


Fig. 8. Relationships between canopy nitrogen (N) concentration and (a) Opt-NDVI, (b) Opt-VI_{opt}, (c) Opt-Cl_{red-edge}, (d) Opt-SIPI, (e) Opt-DCNI, (f) Opt-mNDVI_{blue}, (g) Opt-CCII, (h) Opt-NPDI and (i) Opt-CCCI.

$$NE = \frac{RMSE\{HIs vs. CNC\}}{[d(HIs)/d(CNC)]}$$

where $d(HIs)/d(CNC)$ is the first derivative of the best-fit function of the relationship “HIs vs. CNC”; RMSE is the root mean square error of the best-fit function of this relationship; The lower of the NE indicates the higher of the sensitivity for HIs to CNC of potato.

2.5.2. Stability analysis

The stability of the model is an important reference to evaluate the application potential of the model. In the current study, locations, leaf chlorophyll content and LAI were considered to evaluate the stability of optimized HIs for estimation of potato CNC.

Previous studies have demonstrated that the chlorophyll content is strongly related to crop N status (Croft et al., 2019; Berger et al., 2018). To examine the linearity of different optimized HIs to CNC, the simulated dataset was obtained using the PROSAIL model under the specific conditions, i.e., the chlorophyll content from 10 to 60 $\mu\text{g cm}^{-2}$ at a step of 10 $\mu\text{g cm}^{-2}$ and the other parameters according to the previous studies listed in Table 2 (Kooistra et al., 2016; Duan et al., 2014). Seven thousand valid spectral reflectance were simulated using the PROSAIL model. The Coefficient of Variation (CV) of different optimized HIs and the R^2 of the optimized HIs and chlorophyll content was compared using simulated spectrum to investigate the influence of CNC and LAI

variation on the performance of HIs. A larger R^2 and the lower CV suggests that the optimized HIs have the greater stability in estimating CNC:

$$CV(\%) = \frac{\sigma}{\mu} \times 100$$

where σ is the standard deviation of optimized HIs value, and μ was the mean of optimized HIs value (or its absolute value of μ).

2.5.3. Accuracy analysis

The optimized HIs were evaluated using the independent dataset of farmers’ fields by comparing the R^2 , RMSE and relative error (RE, %) of prediction. A larger R^2 and the lower RMSE and RE suggested the greater accuracy and stability of the model to predict CNC. The RMSE and RE according to the following equations:

$$RMSE = \sqrt{\frac{1}{n} \sum_{i=1}^n (y_i - \hat{y}_i)^2}$$

$$RE(\%) = \frac{RMSE}{\bar{y}} * 100$$

where y , \hat{y}_i and \bar{y} are the measured, predicted and mean values of CNC,

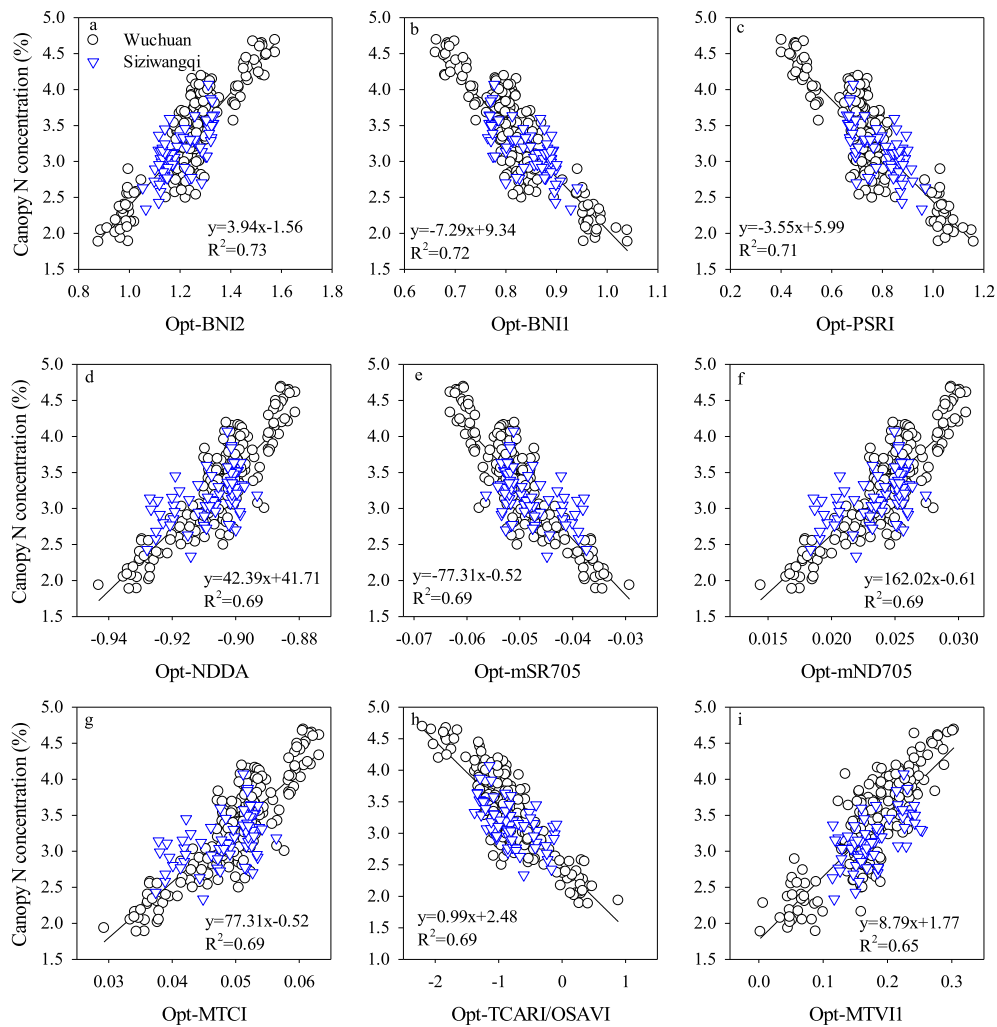


Fig. 9. Relationships between canopy nitrogen (N) concentration and (a) Opt-BNI2, (b) Opt-BNI1, (c) Opt-PSRI (d) Opt-NDDA, (e) Opt-mSR705, (f) Opt-mND705, (g) Opt-MTCI, (h) Opt-TCARI/OSAVI and (i) Opt-MTVII.

respectively, and n is the number of samples.

3. Results

3.1. The relationships between published HIs and CNC

The CNC decreased with the growth stages due to the dilution effect in the calibration and validation datasets (Fig. 1). The results in Figs. 2 and 3 showed that the published HIs explained 2%–53% variation of potato and lost the sensitivity when CNC more than 3.0%.

3.2. Identifying the central bands of optimized HIs

Figs. 4 and 5 illustrate the two-dimension contour and three-dimension slice maps for optimizing two-, three-band and combined HIs. The R^2 changed with different band combinations. The highest R^2 for the best performed HIs and CNC and their sensitive bands were determined based on contour and slice maps. As illustrated in Fig. 6, the Optimized HIs explained 56%–74% variation of potato CNC. The ultraviolet (UV, 300–400 nm) and blue light (B, 450–500 nm) were the main sensitive bands for the two-band HIs in deriving CNC of potato (Fig. 7a), whereas for the three-band HIs, the central sensitive bands were almost located in the UV and green light (G, 520–600 nm) (Fig. 7b). In contrast, the sensitive bands for the combined HIs were mainly found in green wavelengths (Fig. 7c).

3.3. Relationships between optimized hyperspectral indices and CNC

The linear regression models between the best performing optimized HIs and CNC are shown in Figs. 8 and 9. The sensitivity of HIs was greatly increased by band optimum and reduced with the degree of dispersion and location impacts, although the saturation effect for several optimized indices like Opt-NDVI, Opt-CI and Opt-CCII occurred (Figs 3 and 8). The best performing HIs were Opt-mRER and Opt-NPDI with an R^2 of 0.74. Overall, the estimation ability of two-band HIs was inferior to that of three-band and combined HIs.

3.4. Comparison of optimized hyperspectral indices with published indices

The band optimum remarkably increased the performance of HIs in estimating potato CNC (Fig. 10). The R^2 increased by 16%–71% compared to the published HIs. The optimized HIs exhibited different performances even though a similar band optimum algorithm was implemented. In addition to the influence of band selection, the formula formats improved the performance by 3%–18% compared to the worst performed formula formats like RDVI ($R^2 = 0.56$) across years, cultivars and growth stages (Fig. 6).

3.5. Evaluation and validation of optimized hyperspectral indices

The NE increased with the increment of CNC, especially when CNC

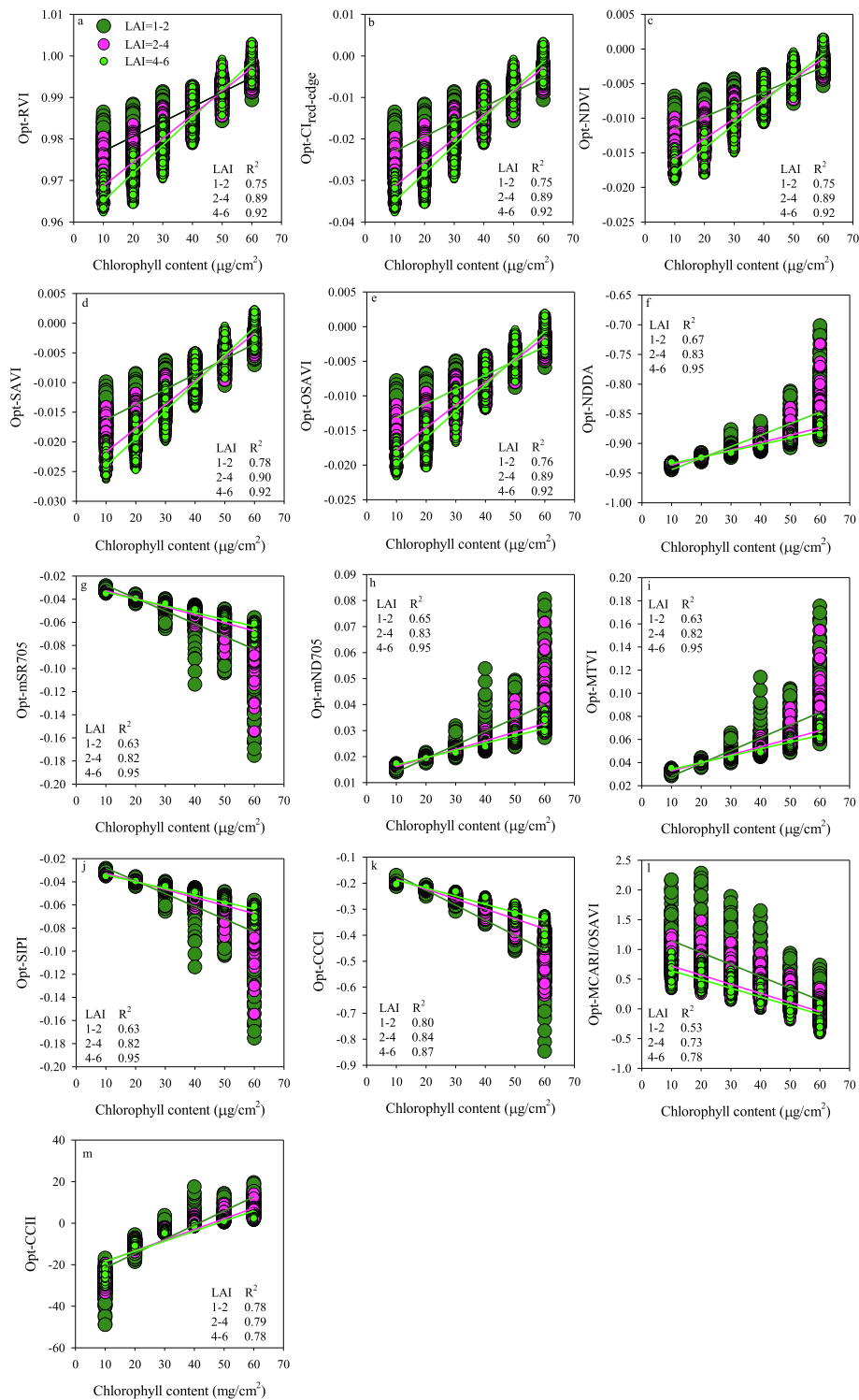


Fig. 12. The effect of leaf area index (LAI) on the relationships between leaf chlorophyll content and the optimized spectral indices.

the optimum band combinations, but also on the formula formats of the HIs. The best performing Optimized HIs were Opt-NDDA, Opt-MTCl, Opt-SIPI, Opt-mSR705, Opt-mND705 with R² at 0.72, RMSE at 0.35% and RE at 8.46%. The second were Opt-MCARI/OSAVI, Opt-CCCI, Opt-CCII, with R² RMSE and RE were 0.66–0.70, 0.35%–0.37%, 8.42–8.78%, respectively (Fig. 14). Overall, the estimated accuracy of the three-band optimized HIs and combined optimized HIs outperformed the two-band Optimized HIs (Figs. 13–15).

4. Discussion

4.1. Variation in sensitive bands of HIs

In the current studies, the sensitive bands to potato CNC mainly located at ultraviolet (340–400 nm) and visible light in blue and green regions (520–600 nm) (Fig. 7). Similarly, the findings for the rice (Stroppiana et al 2009) showed that the optimized index NDI_{opt} (R₅₀₃ nm and R₄₈₃ nm) was the highest sensitivity to CNC from tillering to

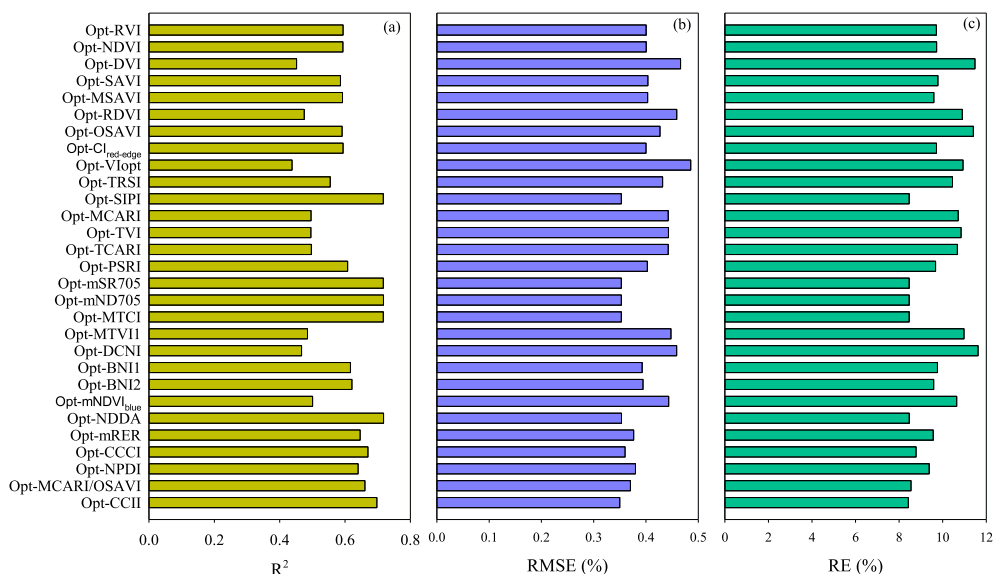


Fig. 13. Comparison of potato canopy nitrogen concentration predictive ability of optimized spectral indices models from farmers' field.

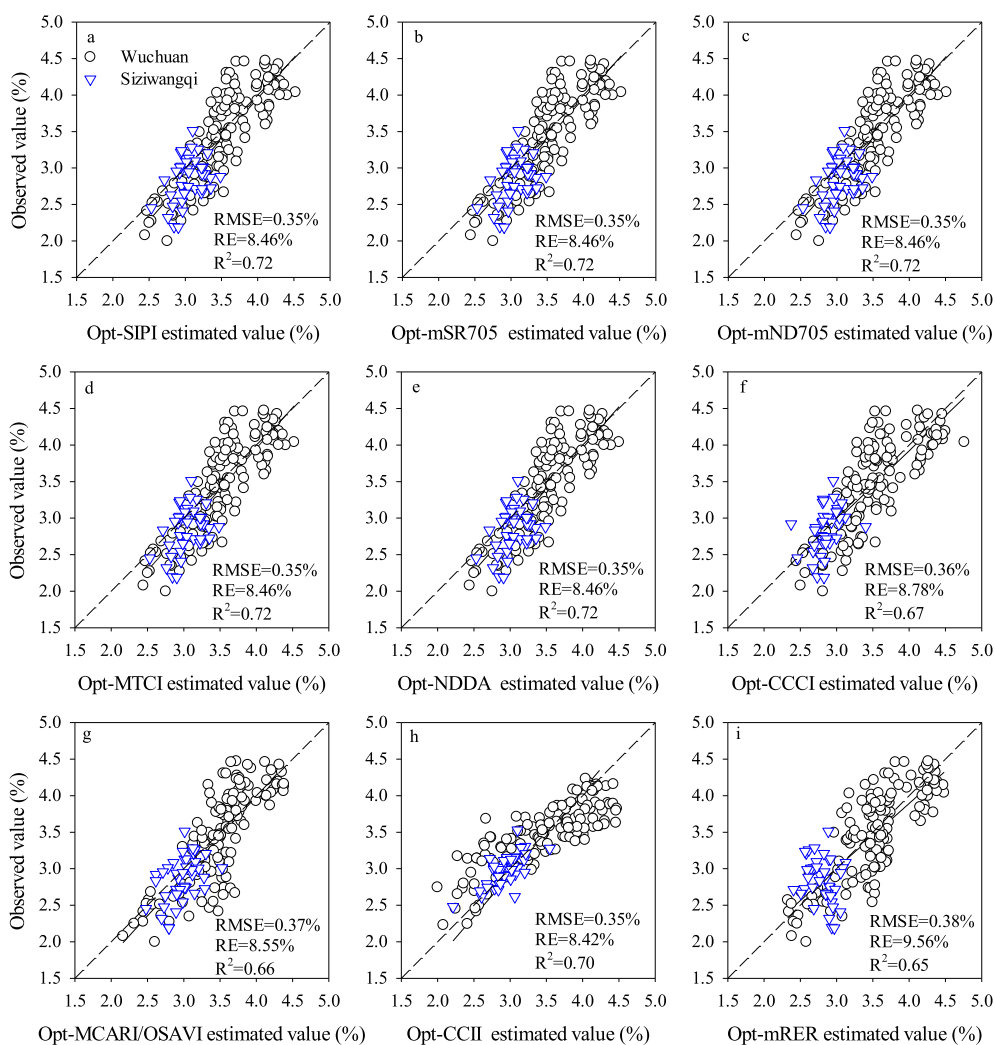


Fig. 14. Relationship between estimated and observed canopy nitrogen concentration (CNC) for the data from farmer's fields (a, b, c, d, e, f, g, h and i stand for Opt-SIPI, Opt-mSR705, Opt-mND705, Opt-MTCI, Opt-NDDA, Opt-CCCI, Opt-MCARI/OSAVI, Opt-CCII and Opt-mRER).

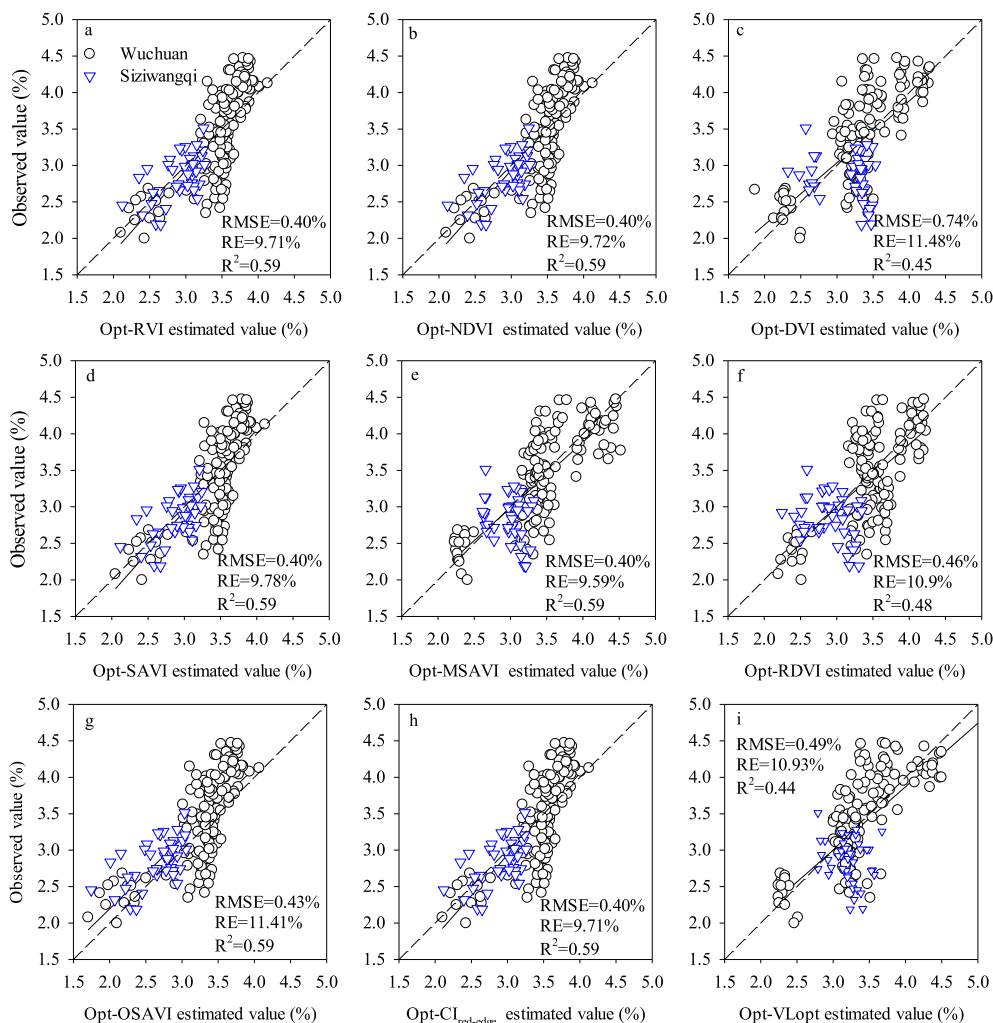


Fig. 15. Relationship between estimated and observed canopy nitrogen concentration (CNC) for the data from farmer's fields (a, b, c, d, e, f, g, h and I stand for Opt-RVI, Opt-NDVI, Opt-DVI, Opt-SAVI, Opt-MSAVI, Opt-RDVI, Opt-OSAVI, Opt-CI_{red-edge} and Opt-VL_{opt}).

booting stages. His photochemical reflectance index (PRI, 531 nm and 570 nm), SR (462 nm and 580 nm) and NDI (478 nm and 506 nm) performed consistently well across all growth stages of rice (Zheng et al., 2018; Yu et al., 2013). In wheat, the ultraviolet, violet and blue were more sensitive bands for CNC based on a common on-farm dataset across site-years, cultivars and growth stages (Li et al., 2010). In contrast, many studies have suggested that the red edge (RE) and near-infrared (NIR) bands play an important role in estimating CNC of wheat (Cheng et al., 2019; Li et al., c, 2014b; Chen et al., 2010), maize (Liu et al., 2019; Li et al., 2014a; Chen et al., 2010) and rice (Yu et al., 2013; Cao et al., 2013; Tian et al., 2011). The red edge based simple ratio and combined HIs performed the best in detecting CNC for rice and winter wheat after the heading stage (Li et al., 2012, 2014c; Yu et al., 2013), and summer maize at the V6, V7 and V10-V12 growth stages (Li et al., 2014a). Overall, Red-edge has been proved to be the best performing bands in single growth stages and the productive stage of the crops, whereas the violet and blue light may perform better in estimating CNC in a variable canopy structure (Fig. 7). These results suggest that the canopy structure and spectral index algorithms greatly influence the selection of sensitive bands. Our results from current and previous studies demonstrated that the CNC-sensitive bands of HIs moved to the short-wavebands due to great changes in canopy structure.

4.2. The influence of HIs optimization algorithm on their performance of CNC estimation

This study showed that identifying optimized band combinations for HIs can significantly improve the performances in deriving potato CNC, which is in agreement with the previous studies in wheat (Li et al., 2014b, c) and rice (Yu et al., 2013; Tian et al., 2011). However, there is a need to evaluate the influence of the HIs algorithms on the estimation performance independent of band position. Therefore, the contribution of the formula formats to the estimation capability through band optimization was compared in this study as well (Figs. 4–6). The results in Figs. 4–6 indicate that the band optimization compensated the formula formats effect for some HIs, e.g., Opt-NDDA, Opt-SIPI, Opt-mSR705 Opt-mND705, Opt-MTVI. Hyperspectral indices formula formats were able to further improve the performance of HIs in extracting CNC of potato by 3%–18% (Fig. 6).

Previous studies have also shown that the three-band HIs are more robust in estimating N nutrient parameters of crops compared to the two-band index (Wang et al., 2012; Li et al., 2014c). Similarly, the three-band spectral indices can overcome the saturation effect and degree of dispersion in estimating CNC of potato plants in the present study (Figs. 8 and 9). In agreement with the findings of Tian et al. (2011), the current studies indicate that introducing a third band (λ_3) in the two-band $R_{\lambda_1}/R_{\lambda_2}$ and $(R_{\lambda_1}-R_{\lambda_2})/(R_{\lambda_1} + R_{\lambda_2})$, i.e., $R_{\lambda_1}/(R_{\lambda_2} + R_{\lambda_3})$, $(R_{\lambda_1}-R_{\lambda_2})/R_{\lambda_3}$, $(R_{\lambda_1}-R_{\lambda_2})/(R_{\lambda_3}-R_{\lambda_2})$ and $(R_{\lambda_1}-R_{\lambda_2})/(R_{\lambda_1} + R_{\lambda_2}-2 \times$

Rλ3), could significantly increase the predicting ability of HIs. In contrast, adding a third band (λ3) in $R\lambda1/(R\lambda2 \times R\lambda3)$ decreased the estimating ability compared to $R\lambda1/R\lambda2$, further suggesting that formula formats have a great influence on the performance of HIs in the estimation of crop CNC.

4.3. Evaluation of optimized HIs

Evaluating the performance of HIs is an essential process to judge their practicability. In addition to the R^2 as a statistical characteristic for the established model, the NE analysis in this study was performed to evaluate the performance of Optimized HIs in estimating potato CNC. The NE of HIs such as Opt-mRER, Opt-NPDI, Opt-BNI1, Opt-BNI2 and Opt-CCCI in CNC were relatively low among 29 optimized HIs (NE: 0.36–0.47) (Fig. 11). Similar to the findings of Li et al. (2012), NPDI and CCCI had lower NE for winter wheat CNC estimation (Fig. 11). The relatively low NE appeared in winter wheat CNC was < 2% (Li et al., 2012), while potato CNC appeared to be < 3% in this study. Similar results have been observed in estimating maize canopy N content (Schlemmer et al., 2013), soybeans fractional vegetation cover (Gitelson, 2013) and plant N uptake for wheat and maize (Hasituya et al., 2020; Li et al., 2014a). Thus, our study confirms that the sensitivity of regression models is affected by both HIs and crop species.

PROSPECT and PROSAIL models are efficient tools to evaluate the performance of HIs (Berger et al., 2018). Le Maire et al. (2004) evaluated the HIs using the PROSPECT model by testing the published HIs from 1973 to 2002, they found the mND705 was a potential spectral index in deriving crop N nutrition index (Li et al., 2018; Xiao et al., 2013). In the current study, the Opt-mSR705 and Opt-mND705 demonstrated better performances for the estimation of potato CNC and chlorophyll content (Figs. 6 and 12). However, the performances of HIs were influenced by LAI. The Opt-NDDA, Opt-mSR705, Opt-mND705, Opt-MTCI and Opt-SIPI showed a better performance compared to other HIs at the late growth period when LAI exceeded the $2 \text{ m}^2/\text{m}^2$, while there was a wide range of CV (Fig. 12 and Table 3), suggesting that they were very sensitive for the variation of external parameters, e.g., LAI, leaf structure parameter and leaf angle. Compared with other optimized HIs, the Opt-CCCI had relative stability in different LAI and leaf chlorophyll content. However, since the absence of the 340–400 nm bands in the simulated dataset does not allow for evaluating the stability of the optimized HIs based on the 340–400 nm bands, e.g., Opt-NPDI, Opt-mRER and Opt-BNI1, therefore, more independent datasets for validation will be needed.

Across-validation dataset from the experiment field was the most commonly used means to evaluate the accuracy of spectral indices in estimating crop parameters (Cummings et al., 2021; Loozen et al., 2020). However, the models always were validated using data used to develop the model. Unlike across-validation, the estimation models based on Optimized HIs were validated using independent datasets acquired from different environmental and management conditions (fields, planting date, growth stages, and N applications, etc.). This study showed that the Opt-NDDA, Opt-mSR705, Opt-mND705, Opt-MTCI and Opt-SIPI had the lowest RMSE and RE% and the RMSE and RE% had a slight increase for Opt-CCCI, Opt-CCII and Opt-MCARI/OSAVI (Figs. 14 and 15). The optimized mRER and NPDI with high R^2 values did not illustrate the best validation, indicating that it is necessary to use an independent dataset for identifying the best performing HIs.

In the current study, a comprehensive evaluation of HIs was employed to develop robust HIs (Figs. 11–15). The new developed HIs can help farmers to effectively perform N management in potatoes at the right rate and at the right time. Another important application of this study is that the results of the optimized HIs in estimating potato CNC provide a theoretical basis for the application of spectral index in hyperspectral satellite images, e.g., the existing EO-1 Hyperion and forthcoming EnMAP. Also, more data from different ecological regions and hyperspectral satellite images should be tested to verify the

robustness, accuracy and application ability of the method.

5. Conclusions

To explore the performance of HI optimization algorithm for deriving CNC of potato plants, 29 formula formats of HIs were selected, and their sensitive center bands were identified across years, N rates, growth stages and cultivars of potato. This study found that the performance of HIs in the estimation of potato CNC was greatly influenced by formula formats and bands optimization, and the sensitive bands for the estimation of potato CNC were from ultraviolet (340–400 nm) to visible light with blue (450–520 nm), and from green (520–600 nm) to red (600–690 nm). The band optimization indices improved the performance by 16%–71%, and could explain 56%–74% of the variations in potato CNC. Based on band optimum, the formula formats resulted in a 3%–18% difference of estimation in CNC among optimized HIs. Optimized HIs Opt-CCCI (600, 582, 650 nm) and Opt-mRER (352, 536, 562 nm) showed the best HIs in estimating potato CNC. In particular, the HI Opt-CCCI showed the best performance on sensibility, accuracy and stability during the estimation of potato CNC across sites, years, N rates, growth stages and cultivars. These findings may be useful for identifying unified HIs to accurately estimate CNC of crops on a large on-farm scale and to provide a basic guideline for the precise management of potato N fertilizer in the future.

CRedit authorship contribution statement

Haibo Yang: Conceptualization, Methodology, Software, Supervision, Validation, Visualization, Writing - original draft, Investigation, Data curation. **Fei Li:** Writing - review & editing. **Yuncai Hu:** Writing - review & editing. **Kang Yu:** Writing - review & editing.

Declaration of Competing Interest

The authors declare that they have no known competing financial interests or personal relationships that could have appeared to influence the work reported in this paper.

Acknowledgments

This research was financially supported by the National Natural Science Foundation of China (41361079), Programs for Key Science and Technology Development of Inner Mongolia in 2019 and 2020 (2019GG248 and 2020GG0038) and Special Fund for Agro-scientific Research in the Public Interest (201503106).

References

- Adão, T., Hruška, J., Pádua, L., Bessa, J., Peres, E., Morais, R., Sousa, J.J., 2017. Hyperspectral imaging: A review on UAV-based sensors, data processing and applications for agriculture and forestry. *Remote Sens.* 9 (11), 1110.
- Berger, K., Atzberger, C., Danner, M., D'Urso, G., Mauser, W., Vuolo, F., Hank, T., 2018. Evaluation of the PROSAIL model capabilities for future hyperspectral model environments: A review study. *Remote Sens.* 10 (1), 85.
- Broge, N.H., Leblanc, E., 2001. Comparing prediction power and stability of broadband and hyperspectral vegetation indices for estimation of green leaf area index and canopy chlorophyll density. *Remote Sens. Environ.* 76 (2), 156–172.
- Chappelle, E.W., Kim, M.S., McMurtrey III, J.E., 1992. Ratio analysis of reflectance spectra (RARS): an algorithm for the remote estimation of the concentrations of chlorophyll a, chlorophyll b, and carotenoids in soybean leaves. *Remote Sens. Environ.* 39 (3), 239–247.
- Croft, H., Arabian, J., Chen, J., Shang, J., Liu, J., 2019. Mapping within-field leaf chlorophyll content in agricultural crops for nitrogen management using Landsat-8 imagery. *Precis. Agric.* 1–25.
- Cao, Q., Miao, Y., Wang, H., Huang, S., Cheng, S., Khosla, R., Jiang, R., 2013. Non-destructive estimation of rice plant nitrogen status with Crop Circle multispectral active canopy sensor. *Field Crop. Res.* 154, 133–144.
- Chen, P., Haboudane, D., Tremblay, N., Wang, J., Vigneault, P., Li, B., 2010. New spectral indicator assessing the efficiency of crop nitrogen treatment in corn and wheat. *Remote Sens. Environ.* 114 (9), 1987–1997.

- Cheng, T., Lu, N., Wang, W., Zhang, Q., Li, D., YAO, X., Liu, S., 2019. Estimation of nitrogen nutrition status in winter wheat from unmanned aerial vehicle based multi-angular multispectral imagery. *Front. Plant Sci.* 10, 1601.
- Clarke, T.R., Moran, M.S., Barnes, E.M., Pinter, P.J., Qi, J., 2001. Planar domain indices: A method for measuring a quality of a single component in two-component pixels. In *IGARSS 2001. Scanning the Present and Resolving the Future. Proceedings. IEEE 2001 International Geoscience and Remote Sensing Symposium (Cat. No. 01CH37217) (Vol. 3, pp. 1279-1281)*. IEEE.
- Cummings, C., Miao, Y., Paiao, G.D., Kang, S., Fernández, F.G., 2021. Corn nitrogen status diagnosis with an innovative multi-parameter crop circle phenom sensing system. *Remote Sens.* 13 (3), 401.
- Daughtry, C.S.T., Walthall, C.L., Kim, M.S., De Colstoun, E.B., McMurtrey III, J.E., 2000. Estimating corn leaf chlorophyll concentration from leaf and canopy reflectance. *Remote Sens. Environ.* 74 (2), 229–239.
- Duan, S., Li, Z., Wu, H., Tang, B., Ma, L., Zhao, E., Li, C., 2014. Inversion of the PROSAIL model to estimate leaf area index of maize, potato, and sunflower fields from unmanned aerial vehicle hyperspectral data. *Int. J. Appl. Earth Observation and Geoinformation* 26, 12–20.
- Dash, Curran., 2004. The MERIS terrestrial chlorophyll index. *Int. J. Remote Sens.* 25 (23), 5403-5413.
- Erdle, K., Mistle, B., Schmidhalter, U., 2011. Comparison of active and passive spectral sensors in discriminating biomass parameters and nitrogen status in wheat cultivars. *Field Crop. Res.* 124 (1), 74–84.
- FAO, 2019. FAOSTAT, Production Database, accessed in 2019. Available at: <http://www.fao.org/faostat/en/#home>.
- Feng, W., Guo, B., Wang, Z., He, L., Song, X., Wang, Y., Guo, T.C., 2014. Measuring leaf nitrogen concentration in winter wheat using double-peak spectral reflection remote sensing data. *Field Crop. Res.* 159, 43–52.
- Feng, W., Guo, B., Zhang, H., He, L., Zhang, Y., Wang, Y., Zhu, Y., Guo, T., 2015. Remote estimation of above ground nitrogen uptake during vegetative growth in winter wheat using hyperspectral red-edge ratio data. *Field Crop. Res.* 180, 197–206.
- Fitzgerald, G., Rodriguez, D., O Leary, G., 2010. Measuring and predicting canopy nitrogen nutrition in wheat using a spectral index—The canopy chlorophyll content index (CCCI). *Field Crop. Res.* 116 (3), 318-324.
- Gitelson, A.A., 2004. Wide dynamic range vegetation index for remote quantification of biophysical characteristics of vegetation. *J. Plant Physiol.* 161 (2), 165–173.
- Gitelson, A.A., 2013. Remote estimation of crop fractional vegetation cover: the use of noise equivalent as an indicator of performance of vegetation indices. *Int. J. Remote Sens.* 34 (17), 6054–6066.
- Gitelson, A.A., Gritz, Y., Merzlyak, M.N., 2003. Relationships between leaf chlorophyll content and spectral reflectance and algorithms for non-destructive chlorophyll assessment in higher plant leaves. *J. Plant Physiology* 160 (3), 271–282.
- Glenn, E.P., Huete, A.R., Nagler, P.L., Nelson, S.G., 2008. Relationship between remotely-sensed vegetation indices, canopy attributes and plant physiological processes: What vegetation indices can and cannot tell us about the landscape. *Sensors* 8 (4), 2136–2160.
- Goffart, J.P., Olivier, M., Frankinet, M., 2008. Potato crop nitrogen status assessment to improve N fertilization management and efficiency: past–present–future. *Potato Res.* 51 (3–4), 355–383.
- Haboudane, D., Miller, J.R., Tremblay, N., Zarco-Tejada, P.J., Dextraze, L., 2002. Integrated narrow-band vegetation indices for prediction of crop chlorophyll content for application to precision agriculture. *Remote Sens. Environ.* 81 (2–3), 416–426.
- Hasituya, Li, F., Elsayed, S., Hu, Y., Schmidhalter, U., 2020. Passive reflectance sensing using optimized two-and three-band spectral indices for quantifying the total nitrogen yield of maize. *Comput. Electron.* 173. <https://doi.org/10.1016/j.compag.2020.105403>.
- Huete, A., 1988. A soil-adjusted vegetation index (SAVI). *Remote Sens. Environ.* 25, 295–309.
- Haboudane, D., Miller, J.R., Pattey, E., Zarco-Tejada, P.J., Strachan, I.B., 2004. Hyperspectral vegetation indices and novel algorithms for predicting green LAI of crop canopies: Modeling and validation in the context of precision agriculture. *Remote Sens. Environ.* 90 (3), 337–352.
- Honkavaara, E., Saari, H., Kaivosoja, J., Pölonen, I., Hakala, T., Litkey, P., Mäkinen, J., Pesonen, L., 2013. Processing and assessment of spectrometric, stereoscopic imagery collected using a lightweight UAV spectral camera for precision agriculture. *Remote Sens.* 5 (10), 5006–5039.
- Jordan, C.F., 1969. Derivation of leaf-area index from quality of light on the forest floor. *Ecology.* 50 (4), 663–666.
- Kasim, N., Sawut, R., Abliz, A., Qingdong, S., Maimuti, B., Yalkun, A., Kahaer, Y., 2018. Estimation of the relative chlorophyll content in spring wheat based on an optimized spectral index. *Photogramm. Eng. Remote Sens.* 84 (12), 801–811.
- Kooistra, L., Clevers, J.G., 2016. Estimating potato leaf chlorophyll content using ratio vegetation indices. *Remote Sens. Lett.* 7 (6), 611–620.
- Lancashire, P.D., Bleiholder, H., Boom, T.V.D., Langeldüddeke, P., Stauss, R., Weber, E., Witzberger, A., 1991. A uniform decimal code for growth stages of crops and weeds. *Ann. Appl. Biol.* 119 (3), 561–601.
- Le Maire, G., François, C., Dufrene, E., 2004. Towards universal broad leaf chlorophyll indices using PROSPECT simulated database and hyperspectral reflectance measurements. *Remote Sens. Environ.* 89 (1), 1–28.
- Li, F., Miao, Y., Feng, G., Yuan, F., Yue, S., Gao, X., Liu, Y., Liu, B., Ustin, S.L., Chen, X., 2014a. Improving estimation of summer maize nitrogen status with red edge-based spectral vegetation indices. *Field Crop. Res.* 157, 111–123.
- Li, F., Miao, Y., Hennig, S.D., Gnyp, M.L., Chen, X., Jia, L., Bareth, G., 2010. Evaluating hyperspectral vegetation indices for estimating nitrogen concentration of winter wheat at different growth stages. *Precis. Agric.* 11 (4), 335–357.
- Li, F., Mistle, B., Hu, Y., Chen, X., Schmidhalter, U., 2014b. Reflectance estimation of canopy nitrogen content in winter wheat using optimised hyperspectral spectral indices and partial least squares regression. *Eur. J. Agron.* 52, 198–209.
- Li, F., Mistle, B., Hu, Y., Chen, X., Schmidhalter, U., 2014c. Optimising three-band spectral indices to assess aerial N concentration, N uptake and aboveground biomass of winter wheat remotely in China and Germany. *ISPRS-J. Photogramm. Remote Sens.* 92, 112–123.
- Li, F., Mistle, B., Hu, Y., Yue, X., Yue, S., Miao, Y., Chen, X., Cui, Z., Meng, Q., Schmidhalter, U., 2012. Remotely estimating aerial N status of phenologically differing winter wheat cultivars grown in contrasting climatic and geographic zones in China and Germany. *Field Crop. Res.* 138, 21–32.
- Li, Z., Jin, X., Yang, G., Drummond, J., Yang, H., Clark, B., Li, Z., Zhao, C., 2018. Remote sensing of leaf and canopy nitrogen status in winter wheat (*Triticum aestivum* L.) based on N-PROSAIL model. *Remote Sens.* 10 (9) <https://doi.org/10.3390/rs10091463>.
- Liu, L., Peng, Z., Zhang, B., Wei, Z., Han, N., Lin, S., Che, H., Cai, J., 2019. Canopy nitrogen concentration monitoring techniques of summer corn based on canopy spectral information. *Sensors* 19 (19), 4123.
- Loozen, Y., Rebel, K.T., de Jong, S.M., Lu, M., Ollinger, S.V., Wassen, M.J., Karssenber, D., 2020. Mapping canopy nitrogen in European forests using remote sensing and environmental variables with the random forests method. *Remote Sens. Environ.* 247 <https://doi.org/10.1016/j.rse.2020.111933>.
- Le Maire, G., François, C., Soudani, K., Berveiller, D., Pontailier, J.Y., Bréda, N., et al., 2008. Calibration and validation of hyperspectral indices for the estimation of broadleaved forest leaf chlorophyll content, leaf mass per area, leaf area index and leaf canopy biomass. *Remote Sens. Environ.* 112 (10), 3846–3864.
- Peñuelas, J., Baret, F., Filella, I., 1995. Semi-empirical indices to assess carotenoids/chlorophyll a ratio from leaf spectral reflectance. *Photosynthetica* 31 (2), 221–230.
- Prey, L., Schmidhalter, U., 2019. Sensitivity of Vegetation Indices for estimating vegetative N status in winter wheat. *Sensors* 19 (17), 3712.
- Qi, J., Chehbouni, A., Huete, A.R., Kerr, Y.H., Sorooshian, S., 1994. A modified soil adjusted vegetation index. *Remote Sens. Environ.* 48 (2), 119–126.
- Rondeaux, G., Steven, M., Baret, F., 1996. Optimization of soil-adjusted vegetation indices. *Remote Sens. Environ.* 55 (2), 95–107.
- Rouse, J.W., Haas, R.H., Deering, D.W., Schell, J.A., Harlan, J.C., 1974. Monitoring the Vernal Advancement and Retrogradation (Green Wave Effect) of Natural Vegetation. NASA/GSFC Type III Final Report, Greenbelt, Md, p. 371.
- Roujean, J.L., Breon, F.M., 1995. Estimating PAR absorbed by vegetation from bidirectional reflectance measurements. *Remote Sens. Environ.* 51 (3), 375–384.
- Reyniers, M., Walvoort, D.J., De Baardemaaker, J., 2006. A linear model to predict with a multi-spectral radiometer the amount of nitrogen in winter wheat. *Int. J. Remote Sens.* 27 (19), 4159–4179.
- Schmidhalter, U., 2005. Development of a quick on-farm test to determine nitrate levels in soil. *J. Plant Nutr. Soil Sci.* 168 (4), 432–438.
- Schlemmer, M., Gitelson, A., Schepers, J., Ferguson, R., Peng, Y., Shanahan, J., Rundquist, D., 2013. Remote estimation of nitrogen and chlorophyll contents in maize at leaf and canopy levels. *Int. J. Appl. Earth Observation Geoinformation* 25, 47–54.
- Sims, D.A., Gamon, J.A., 2002. Relationships between leaf pigment content and spectral reflectance across a wide range of species, leaf structures and developmental stages. *Remote Sens. Environ.* 81 (2–3), 337–354.
- Stroppiana, D., Boschetti, M., Brivio, P.A., Bocchi, S., 2009. Plant nitrogen concentration in paddy rice from field canopy hyperspectral radiometry. *Field Crop. Res.* 111 (1–2), 119–129.
- Tang, J., Xiao, D., Wang, J., Fang, Q., Zhang, J., Bai, H., 2021. Optimizing water and nitrogen managements for potato production in the agro-pastoral ecotone in North China. *Agric. Water Manage.* 253 <https://doi.org/10.1016/j.agwat.2021.106857>.
- Tucker, C.J., 1979. Red and photographic infrared linear combinations for monitoring vegetation. *Remote Sens. Environ.* 8 (2), 127–150.
- Thenkabail, P.S., Smith, R.B., De Pauw, E., 2000. Hyperspectral vegetation indices and their relationships with agricultural crop characteristics. *Remote Sens. Environ.* 71 (2), 158–182.
- Tian, Y., Yao, X., Yang, J., Cao, W., Hannaway, D.B., Zhu, Y., 2011. Assessing newly developed and published vegetation indices for estimating rice leaf nitrogen concentration with ground-and space-based hyperspectral reflectance. *Field Crop. Res.* 120 (2), 299–310.
- Verrelst, J., Malenovsky, Z., Van der Tol, C., Camps-Valls, G., Gastellu-Etchegorry, J.P., Lewis, P., North, P., Moreno, J., 2019. Quantifying vegetation biophysical variables from imaging spectroscopy data: a review on retrieval methods. *Surv. Geophys.* 40 (3), 589–629.
- Víña, A., Gitelson, A.A., 2005. New developments in the remote estimation of the fraction of absorbed photosynthetically active radiation in crops. *Geophys. Res. Lett.* 32 (17). <https://doi.org/10.1029/2005GL023647>.
- Wang, W., Yao, X., Yao, X., Tian, Y., Liu, X., Ni, J., Cao, W., Zhu, Y., 2012. Estimating leaf nitrogen concentration with three-band vegetation indices in rice and wheat. *Field Crop. Res.* 129, 90–98.
- Wang, N., Reidsma, P., Pronk, A.A., de Wit, A.J.W., van Ittersum, M.K., 2018. Can potato add to China's food self-sufficiency? The scope for increasing potato production in China. *Eur. J. Agron.* 101, 20–29.
- Wang, N., Reidsma, P., Wang, Z.Q., van Ittersum, M.K., 2019. Synergy or trade-off? A framework and application to benchmark yield, quality and revenue of potato production. *Field Crop. Res.* 240, 116–124.
- Xiao, Y., Zhao, W., Zhou, D., Gong, H., 2013. Sensitivity analysis of vegetation reflectance to biochemical and biophysical variables at leaf, canopy, and regional scales. *IEEE Trans. Geosci. Remote Sens.* 52 (7), 4014–4024.

- Yu, K., Lenz-Wiedemann, V., Chen, X., Bareth, G., 2014. Estimating leaf chlorophyll of barley at different growth stages using spectral indices to reduce soil background and canopy structure effects. *ISPRS-J. Photogramm. Remote Sens.* 97, 58–77.
- Yu, K., Li, F., Gnyp, M.L., Miao, Y., Bareth, G., Chen, X., 2013. Remotely detecting canopy nitrogen concentration and uptake of paddy rice in the Northeast China Plain. *ISPRS-J. Photogramm. Remote Sens.* 78, 102–115.
- Zarco-Tejada, P.J., Miller, J.R., Morales, A., Berjón, A., Agüera, J., 2004. Hyperspectral indices and model simulation for chlorophyll estimation in open-canopy tree crops. *Remote Sens. Environ.* 90 (4), 463–476.
- Zhao, C., Wang, Z., Wang, J., Huang, W., 2012. Relationships of leaf nitrogen concentration and canopy nitrogen density with spectral features parameters and narrow-band spectral indices calculated from field winter wheat (*Triticum aestivum* L.) spectra. *Int. J. Remote Sens.* 33 (11), 3472–3491.
- Zheng, H., Cheng, T., Li, D., Yao, X., Tian, Y., Cao, W., Zhu, Y., 2018. Combining unmanned aerial vehicle (UAV)-based multispectral imagery and ground-based hyperspectral data for plant nitrogen concentration estimation in rice. *Front. Plant Sci.* 9, 936.
- Zhang, N., Yang, G., Pan, Y., Yang, X., Chen, L., Zhao, C., 2020. A Review of advanced technologies and development for hyperspectral-based plant disease detection in the past three decades. *Remote Sens.* 12 (19), 3188.